Clinical and Experimental Pancreatic Islet Transplantation to Striated Muscle

Establishment of a Vascular System Similar to That in Native Islets

Gustaf Christoffersson,[1] Johanna Henriksnäs,[1] Lars Johansson,[2] Charlotte Rolny,[3] Håkan Ahlström,[2] José Caballero-Corbalan,[2] Ralf Segersvärd,[4] Johan Permert,[4] Olle Korsgren,[2] Per-Ola Carlsson,[1,5] and Mia Phillipson[1]

OBJECTIVE—Curing type 1 diabetes by transplanting pancreatic islets into the liver is associated with poor long-term outcome and graft failure at least partly due to inadequate graft revascularization. The aim of the current study was to evaluate striated muscle as a potential angiogenic site for islet transplantation.

RESEARCH DESIGN AND METHODS—The current study presents a new experimental model that is found to be applicable to clinical islet transplantation. Islets were implanted into striated muscle and intraislet vascular density and blood flow were visualized with intravital and confocal microscopy in mice and by magnetic resonance imaging in three autotransplanted pancreatectomized patients. Mice were rendered neutropenic by repeated injections of Gr-1 antibody, and diabetes was induced by alloxan treatment.

RESULTS—Contrary to liver-engrafted islets, islets transplanted to mouse muscle were revascularized with vessel densities and blood flow entirely comparable with those of islets within intact pancreas. Initiation of islet revascularization at the muscular site was dependent on neutrophils, and the function of islets transplanted to muscle was proven by curing diabetic mice. The experimental data were confirmed in autotransplanted patients where higher plasma volumes were measured in islets engrafted in forearm muscle compared with adjacent muscle tissue through high-resolution magnetic resonance imaging.

CONCLUSIONS—This study presents a novel paradigm in islet transplantation whereby recruited neutrophils are crucial for the functionally restored intraislet blood perfusion following transplantation to striated muscle under experimental and clinical situations. *Diabetes* **59:2569–2578, 2010**

From the [1]Department of Medical Cell Biology, Uppsala University, Uppsala, Sweden; the [2]Department of Oncology, Radiology and Clinical Immunology, Uppsala University, Uppsala, Sweden; the [3]Department of Genetics and Pathology, Uppsala University, Uppsala, Sweden; the [4]Department for Clinical Science, Intervention and Technology, Karolinska Institutet, Stockholm, Sweden; and the [5]Department of Medical Sciences, Uppsala University, Uppsala, Sweden.

Corresponding author: Mia Phillipson, mia.phillipson@mcb.uu.se.

Transplantation of pancreatic tissue is today the only curative treatment for type 1 diabetes. Clinically, either the entire pancreas is transplanted into the abdominal cavity or isolated insulin producing islets of Langerhans are implanted into the liver through infusion via the portal vein. The former procedure is highly successful; the graft functions well following transplantation. However, it requires extensive surgery, whereas the latter procedure is attractive because only minor surgery is required in conscious recipients. Unfortunately, both function and survival of intrahepatically transplanted islets deteriorate with time (1). Delayed and insufficient islet revascularization (2), gluco- and lipotoxicity (3), presence of an instant blood-mediated inflammatory reaction (4,5), and toxicity of the immunosuppressive drugs present in high concentrations in the portal blood (6,7) are all factors believed to contribute to graft failure at this site.

Native islets are highly vascularized, with blood perfusions ten times higher than in the exocrine pancreas (8,9). The islet microvasculature consists of a dense glomerular-like capillary network. A specific perfusion order of the different endocrine cell types has been shown in islets of Langerhans (10–15), enabling intraislet cell communication and further demonstrating the importance of a refined and adequate intraislet blood flow for normal islet function.

Many of the factors contributing to poor islet function are associated with the liver as the site for engraftment (3,5,6,16,17), and for this reason other sites are now being investigated. The intramuscular site has attracted recent interest as a result of positive long-term outcome of autotransplantation of parathyroid glands to the brachioradialis muscle (18). Indeed, in a recent case report, we documented a successful 2-years follow-up of a child receiving autotransplanted islets into muscle (19).

Myeloid-derived leukocytes have recently been shown to be involved in muscle healing and regeneration including angiogenesis (20,21); we therefore hypothesized that leukocytes may also be involved in the engraftment and revascularization of transplanted islets to muscle. To address this hypothesis, in addition to evaluation of striated muscle as a potential angiogenic site for islet transplantation, an in vivo mouse model was developed that enables studies of leukocyte–endothelial cell interactions and blood flow during revascularization of transplanted

islets by intravital and confocal microscopy. Long-term islet function and survival following transplantation to muscle were evaluated in diabetic recipients. The results achieved in the experimental model were thereafter validated in patients receiving islets autotransplanted to muscle following pancreatectomy with a sophisticated magnetic resonance imaging technique.

RESEARCH DESIGN AND METHODS

Male C57Bl/6 mice (25–30 g ([B&K Universal]) and C57Bl/6 nu/nu mice (25–30 g [Taconic M&B]) were used. Experiments were approved by the Uppsala Laboratory Animal Ethical Committee. An online appendix describes additional methods (http://diabetes.diabetesjournals.org/cgi/content/full/db10-0205/DC1).
Islet isolation and transplantation to mice. Mouse islets of Langerhans were isolated and cultured over night as previously described (22). Human islets from five heart-beating female donors (age 57 ± 7 years) were isolated and cultured as previously described (23). Islets were fluorescently labeled immediately before transplantation with the intracellular probes Celltracker Blue CMAC or Celltrace Far Red DDAO (Invitrogen), depending on the type of imaging performed later. For transplantation into the cremaster muscle (surrounding the testis) of nondiabetic mice, 5–20 islets in suspension were, by the use of a butterfly needle (25G), repeatedly injected subfascially at different spots to allow for single islet engraftment. For transplantation to the liver of nondiabetic mice, 200 islets were infused via the portal vein.

Diabetic mice (injected with 75 mg/kg i.v. alloxan; Sigma-Aldrich) had plasma glucose concentrations of 25.8 ± 1.0 mmol/l on the day of transplantation. A suspension with 300 islets was injected superficially between abdominal external oblique muscle fibers (on the side of the abdomen) or infused into the portal vein to the liver. Plasma glucose levels <11.1 mmol/l were deemed normalized, and mice were killed if blood glucose levels were >20 mmol/l 7 days posttransplantation.
Intravital microscopy. The cremaster muscles of isoflurane-anaestetized (Abbott) mice with implanted islets were prepared for intravital microscopy as previously described (24). A catheter in the femoral artery allowed retrograde infusion close intra-arterially to the muscle. An intravital microscope (Leica Microsystems DM5000B equipped with a Hamamatsu Orca-R2 CCD camera and HCX Apo L 20×/0.50W and 40×/0.80W objectives; Volocity software) was used to visualize the microcirculation of transplanted islets and surrounding muscle. Recordings were made for analysis of adherent (stationary for >30 s within 100 μm length of venule in 3 min) and emigrated leukocytes (cells in the extravascular space per field of view [0.05 mm^2]).

Laser scanning confocal microscopy (Nikon C-1 with Plan Fluor ELWD 20×/0.45 and 40×/0.60 objectives; Nikon EZ-C1 software), spinning disk confocal microscopy (Olympus BX51/Quorum WaveFx with a Hamamatsu C9100-13 EMCCD camera and an XLUM Plan F1 20×/0.95W objective; Volocity software), or multiphoton microscopy (Olympus FV300/Chameleon ti:sapphire laser with a 40×/0.80W objective and Olympus FluoView and ImageJ software or Zeiss 710 NLO with a Plan-Apo 20×/1.0W objective; Zeiss Zen software) was performed after intra-arterial injection of 25 μg Alexa Fluor 555 or 594 anti–CD31 monoclonal antibody (mAb) (clone 390; eBioscience) to stain endothelium and 15 μg fluorescein isothiocyanate (FITC) anti–Gr-1 mAb (clone RB6–8C5; eBioscience) to stain neutrophils.
Vessel density and functionality. Paraffin sections of transplants were stained for insulin with anti-insulin antibody (Fitzgerald) and for endothelium with the lectin Bandeiraea simplicifolia-1 (BS-1) (Sigma-Aldrich) (supplemental Figs. 1 and 2). Vessel functionality within grafts was studied through intrajugular injection of 100 μg soybean agglutinin (SBA) lectin, which stains endothelium and allows for detection of perfused vessels. Endothelium was stained in cryosections with anti-CD31 mAb (conjugated to Alexa Fluor 555), and nuclei were stained with Hoechst 33342 (Invitrogen).
Neutrophil depletion. Mice were rendered neutropenic by intraperitoneal injections of anti–Gr-1 (clone RB6-8C5; eBioscience). Immunoglobulin G (IgG) isotype antibody (eBioscience) was injected in controls. One day prior to transplantation (day zero), 150 μg was injected; an additional 150 μg was injected on day three. Determination of treatment efficiency was made by blood analysis and differential count. Total leukocyte counts were reduced by 50% ($8.2 \pm 1.0 \times 10^9/l$ vs. $4.1 \pm 0.6 \times 10^9/l$), and neutrophil counts were reduced by 80% ($19.2 \pm 5.2 \times 10^8/l$ vs. $4.2 \pm 1.2 \times 10^8/l$). No Gr-1–postive cells were found nearby the grafts in Gr-1 antibody–treated animals.
Clinical intramuscular islet autotransplantation. The study was approved by the Regional Ethics Board, Uppsala, Sweden, and was performed in accordance with local institutional and Swedish national rules and regulations.

Three patients (two men and one woman) with intraductal papillary mucinous neoplasm underwent total pancreatectomy with a Whipple proce-

TABLE 1
Islet characterization and patient metabolic status before and after the operation and after transplantation and islet characterization

	Subject 1	Subject 2	Subject 3
Preoperation			
A1C (%)	6.7	5.0	6.1
F-PG (mmol/l)	6.6	6.6	5.4
Stimulated CP (ng/ml)	0.90	3.60	6.30
Postoperation			
Stimulated CP (ng/ml)	<0.12	<0.12	<0.12
Islet isolation			
Islet yield (%)	286,957	202,174	250,435
Purity (%)	80	26	32
Volume (μl)	825	2,725	1,800
Stimulation index			
(16.7/1.67 mmol/l)	11.8	>25	>25
Content (ng/ng DNA)	9.945	0.541	0.743
ADP/ATP ratio	0.050	0.050	0.060
Posttransplantation			
A1C (%)	7.9	8.0	7.0
F-PG (mM)	7.4	9.3	9.7
Insulin needs			
(IU/kg body wt)	0.45	0.51	0.62
Basal CP (ng/ml)	0.39	<0.12	<0.12
Stimulated CP (ng/ml)	1.32	0.45	0.39

CP, C-peptide; F-PG, fasting plasma glucose; IE, islet equivalent.

dure and autologous intramuscular islet transplantation (Table 1). Ex vivo the pancreas was immediately perfused with cold (4°C) University of Wisconsin solution and shipped to the islet isolation laboratory of the Nordic Network for Clinical Islet Transplantation (cold ischemic time <2 hours). Islet isolation was performed as previously described (23), and islets were maintained in culture for 24 h before characterization (supplemental Table 1).

Absence of functioning endocrine pancreatic tissue before islet transplantation was confirmed in all patients by lack of C-peptide (Table 1) (25). Under brachial plexus anesthesia, islets in volumes of 50–100 μl were injected into the muscle fibers of the brachioradialis muscle (in the forearm) with the help of a central venous catheter (Secalon-T, 16G, 130 mm; BD Biosciences). Islet graft function after transplantation was assessed by circulating C-peptide (Table 1).

The subjects were scanned 3–6 months posttransplantation using a 1.5 T clinical magnetic resonance scanner (Gyroscan Intera; Philips Medical Systems). The body coil was used for radio frequency transmission and a 45-mm circular linear coil for radio frequency reception. High-resolution axial images were obtained using a T1-weighted three-dimensional gradient echo acquisition with 32 slices, (in-plane resolution of 200×200 μm^2 and a slice thickness of 1.0 mm; TR/TE/flip 16/5/10).
Statistics. Data are means $\pm$ SEM. Paired and unpaired two-tailed Student t tests were used to compare between groups.

RESULTS

This study used a novel experimental model where isolated pancreatic islets are transplanted into the mouse cremaster muscle for ease of visualization. The reestablished circulation to the transplanted tissue was studied by transillumination, epifluorescence, spinning disk, laser scanning confocal and multiphoton microscopy, and the functionality of intramuscularly engrafted islets was tested in diabetic recipients. For translational purposes, ultrahigh resolution magnetic resonance imaging was performed on autotransplanted islets engrafted in the brachioradialis muscle of patients in order to evaluate islet revascularization through measurements of plasma volume in transplanted islets versus surrounding muscle tissue.

Normalized intraislet vascular density after islet transplantation to striated muscle. Islets syngeneically transplanted to the cremaster muscle of nondiabetic mice rapidly became vascularized and showed functional intraislet blood vessels already at 3–5 days after transplantation, as confirmed by close intra-arterial injection of fluorescently labeled anti-CD31 mAb (Fig. 1A), with a vessel density of 407 ± 94 vessels/mm^2 (Fig. 1D). Following these early events, the vasculature continued to develop and, 2 weeks after transplantation, had the characteristic glomerular-like vascular network (Fig. 1B) seen in native islets (Fig. 1C). Two to four weeks posttransplantation, intraislet vascular densities had increased threefold ($1,187 \pm 187$ and $1,162 \pm 120$ vessels/mm^2, respectively) and were similar to those observed in islets in intact pancreas ($1,074 \pm 174$ vessels/mm^2) (Fig. 1D). Imaging of islet vasculature with deeply penetrating multiphoton microscopy 2 weeks posttransplantation revealed a complete vascular network throughout the islet (supplemental Video 1). When intraislet vessel densities were analyzed in islets transplanted intraportally to the liver of nondiabetic mice, vessels surrounding the whole islets were detected but no intraislet vessels could be found 2 or 4 weeks after transplantation ($n = 7$ mice) (supplemental Fig. 1). Transplanted islets at both sites stained positive for insulin (supplemental Fig. 1). The intraislet capillary diameter was enlarged 3–5 days posttransplantation to muscle but was normalized to diameters found in islets in intact pancreas after 2 weeks (Fig. 1E) as previously reported (26).

High vascular densities after human islet transplantation to mouse striated muscle. To investigate whether the improved vascularization of mouse islets transplanted to muscle also applied to human islets, human islets were implanted into the cremaster muscle of immune incompetent mice (nu/nu). For logistic reasons, the human islets were cultured for an average of 4 days prior to transplantation and, for comparison, mouse islets were also cultured for an equal period of time. Four weeks posttransplantation, human islets were highly vascularized with an intraislet vascular density comparable with that of cultured mouse islets (Fig. 1F). Intravital and confocal microscopy showed functional vessels in transplanted human islets, although the vessel structure was somewhat different than that observed for transplanted mouse islets: intraislet capillary diameters were more heterogeneous (9–20 μm) and had a differently organized, less glomerular-like vasculature (Fig. 1G and supplemental Video 2) than that observed in mouse islets (Fig. 1B and C). The number of remnant endothelial cells has been reported to decrease with time in culture (27). However, the vascular densities of mouse islets cultured for 4 days were not significantly lower compared with mouse islets cultured overnight (942 ± 50 and $1,162 \pm 120$ vessels/mm^2, respectively) (Fig. 1D and F), suggesting that the decreased number of remnant donor endothelial cells does not affect the vascularization 4 weeks after transplantation.

Functionally restored vessels after islet transplantation to striated muscle. The functionality of the newly formed vessels within transplanted islets was investigated by intravenous injections of fluorescent SBA lectin (Fig. 2A and B), which ensures endothelial staining of perfused vessels only. After termination of experiments, muscle cryosections were stained for endothelial cells with anti-CD31 mAb and the numbers of lectin- and CD31-positive vessels were analyzed. In islets transplanted to striated muscle and in islets in the intact pancreas, close to 100% of the CD31-positive vessels were also positive for lectin (Fig. 2C–E), indicating that nearly all vessels were indeed perfused. Contrary, the very few CD31-positive cells that could be found within islets transplanted to liver showed low staining overlap with intravenously administered lectin, suggesting mainly nonfunctional vessels, i.e., possibly remnant donor endothelial cells (Fig. 2F).
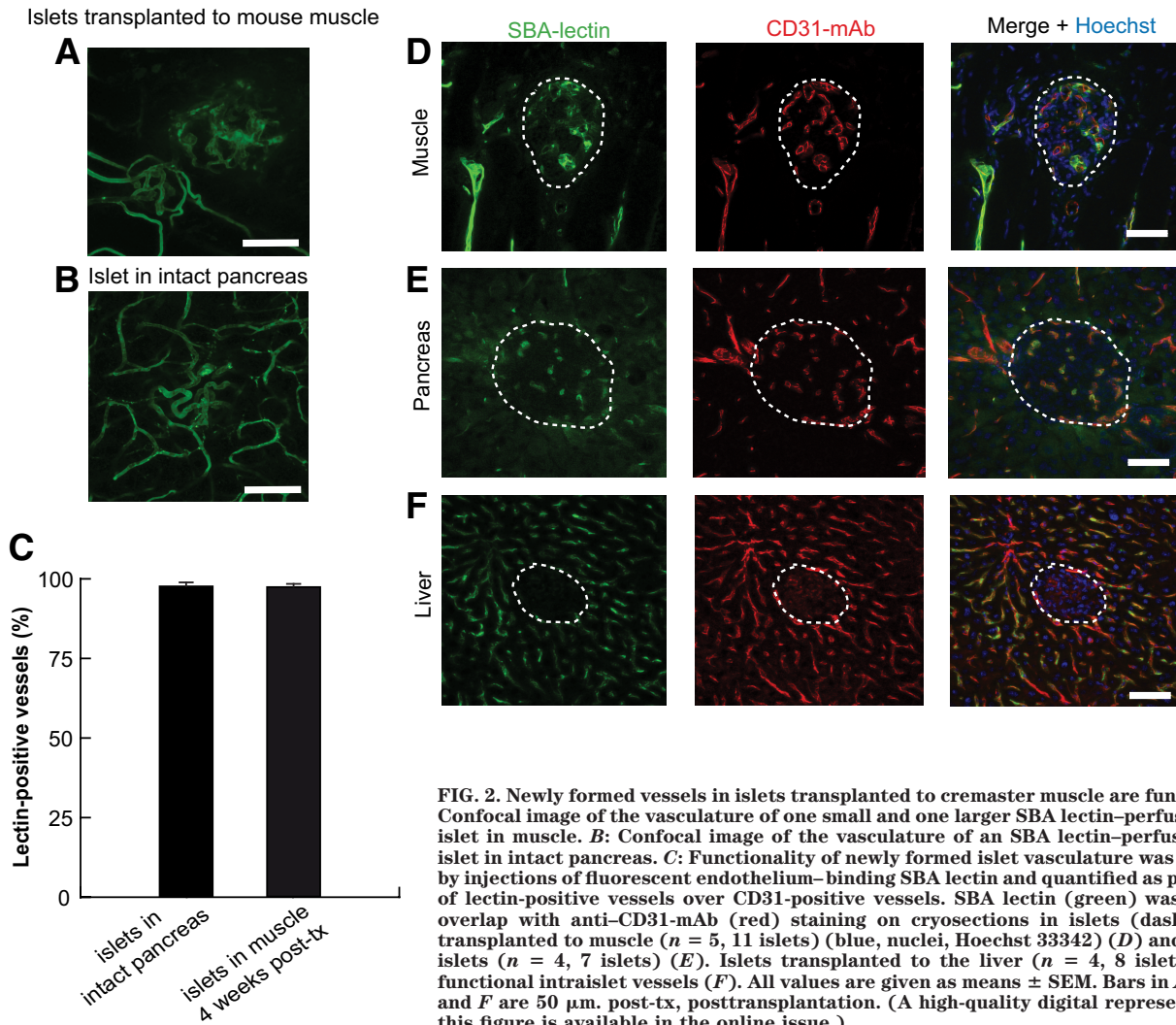
Blood flow organization in transplanted mouse and human islets. In rodents, the β-cell core of the islet receives blood before the endocrine cell types in the islet mantle: the α-, δ- and PP-cells (i.e., β-α-δ blood flow pattern) (14,28). To investigate the blood flow pattern following transplantation to muscle, fluorescently labeled dextran was injected close intra-arterially and islet blood flow was recorded by epifluorescence microscopy. Indeed, 4 weeks after transplantation, mouse islets in muscle were perfused from the core outwards because the fluorescent signal was initially observed in the central part of the islet (supplemental Fig. 3A, C, and E). This indicates that transplantation and revascularization of islets at the intramuscular site do not change the inherent perfusion pattern.

Contrary to the mouse islet organization described above, human islets have a differently organized distribution of endocrine cells throughout the islet with clusterized subunits (29–32). Blood flow recordings of human islets transplanted to the cremaster muscle of nu/nu mice during fluorescent dextran injections revealed a differently organized perfusion pattern (4 weeks posttransplantation [supplemental Fig. 2B, D, and F]). While the blood perfusion of mouse islets was directed from the core and outward, human islets were observed to be perfused from one side to the other in a more polarized manner and no core-to-mantle perfusion could be detected. This implies that the blood flow of pancreatic islets differs between species and that the inherent organization of different endocrine cell types within the islet influences revascularization and thereby gives the perfusion order.

Increased leukocyte-endothelial cell interactions in grafts. Syngeneic transplantation is not associated with acquired immune cell activation or concomitant graft rejection because donor and recipient share the same genetic background. However, intravital microscopy of newly formed vasculature in these grafts exposed interactions between circulating leukocytes and endothelial cells within the islet capillaries and in the venules draining the islets but not at sites receiving sham injections of islet culture medium. Significantly more leukocytes adhered in venules draining islets compared than in venules draining adjacent muscle tissue 3–5 days posttransplantation (Fig. 3A), and emigrated leukocytes were found in the perivascular tissue in the proximity of recently transplanted islets (Fig. 3B). In vivo fluorescent staining of leukocytes with an acute injection of low-dose anti–Gr-1 mAb intra-arterially revealed that the majority of recruited leukocytes were Gr-1–positive leukocytes (Fig. 3C). The number of recruited leukocytes decreased with time after transplantation, indicating a role of leukocyte recruitment during the initial stages of reestablishment of circulation (Fig. 3B). Gr-1–positive leukocytes have been shown to be involved in muscle healing and regeneration (20,21); we therefore investigated their involvement in the revascularization of transplanted islets. Transplantation of islets to neu-
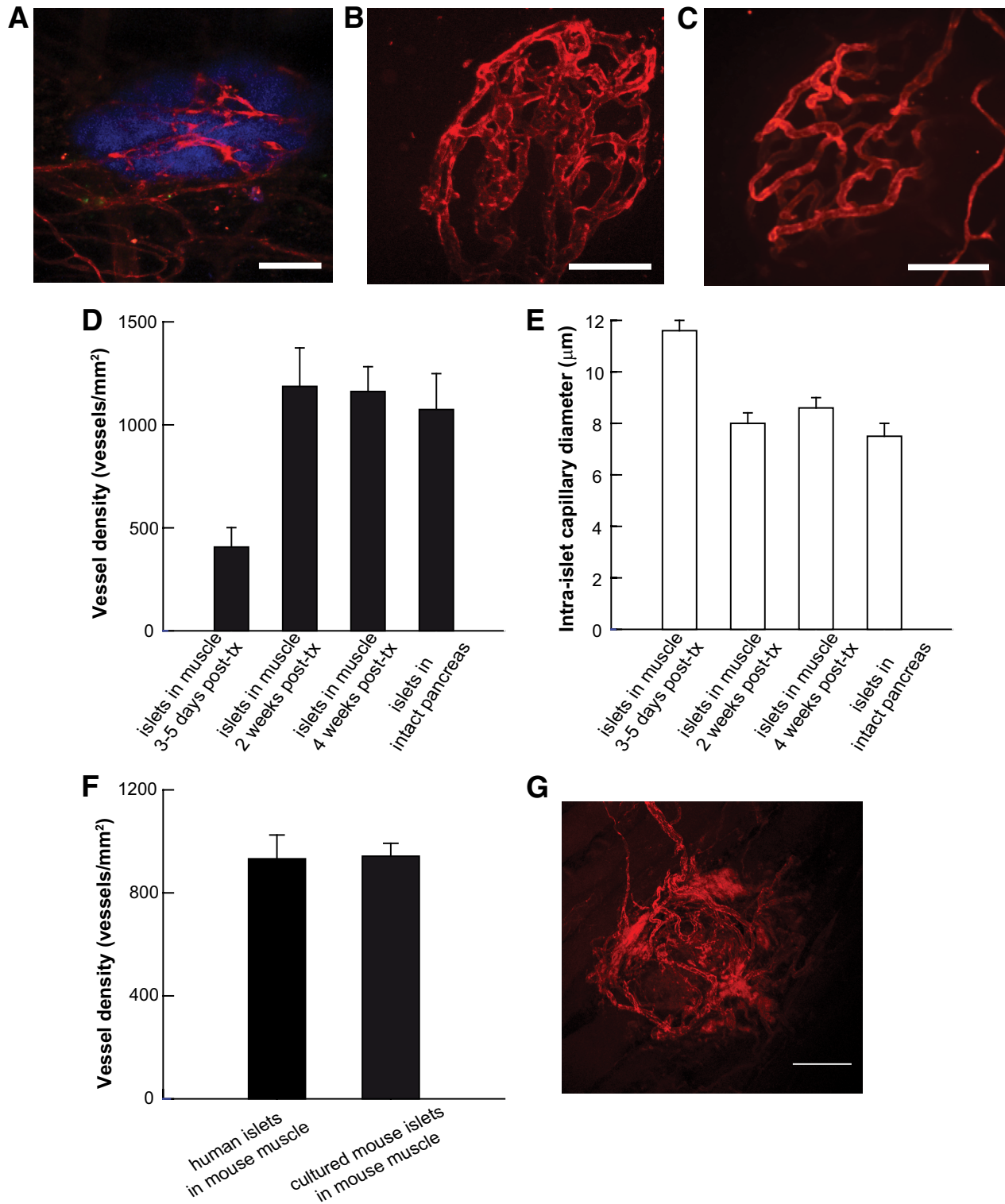
FIG. 1. Islets transplanted to mouse muscle revascularize rapidly and completely. *A*: Three to five days after transplantation, islets in the cremaster muscle have functional intraislet blood vessels: confocal image of a mouse islet (blue; Celltracker) in the cremaster muscle 5 days posttransplantation (post-tx), with ingrowing blood vessels (red; anti–CD31-mAb perfused intra-arterially in vivo). *B*: Two weeks after transplantation, a dense, glomerular-like vascular system developed: multiphoton microscopy image of the vasculature of a transplanted mouse islet in muscle (anti–CD31-mAb). *C*: The vascular density and architecture were, at 2 and 4 weeks posttransplantation, comparable with native islets in the pancreas: spinning disk confocal image of islet vasculature in mouse pancreas (anti–CD31-mAb). *D*: Vessel density in islets transplanted into mouse muscle at 3–5 days ($n = 4$), 2 weeks ($n = 4$), and 4 weeks ($n = 6$) after transplantation compared with the density observed in islets in intact pancreas ($n = 4$). Islets transplanted into the liver did not have any intraislet vessels at these time points ($n = 7$). *E*: Intraislet capillary diameter of transplanted mouse islets is increased shortly after transplantation (3–5 days; $n = 5$, 3 capillaries/islet) but reaches values comparable with native islet capillaries ($n = 3$, 3 capillaries/islet) at 2 weeks posttransplantation ($n = 4$, 3 capillaries/islet). *F*: The vascular densities of human islets transplanted to mouse muscle ($n = 4$) were at the same high level as mouse islets cultured for the same number of days ($n = 3$). *G*: Human islets transplanted to muscle of nu/nu mice had a well-developed intraislet vascular system 4 weeks after transplantation: multiphoton microscopy image of human islet vasculature (anti–CD31-mAb). All values are given as means ± SEM. Bars in *A*, *B*, *C*, and *G* are 50 μm. (A high-quality digital representation of this figure is available in the online issue.)

Islets transplanted to mouse muscle

A

B Islet in intact pancreas

C

SBA-lectin   CD31-mAb   Merge + Hoechst

D Muscle

E Pancreas

F Liver

FIG. 2. Newly formed vessels in islets transplanted to cremaster muscle are functional. *A*: Confocal image of the vasculature of one small and one larger SBA lectin–perfused mouse islet in muscle. *B*: Confocal image of the vasculature of an SBA lectin–perfused mouse islet in intact pancreas. *C*: Functionality of newly formed islet vasculature was evaluated by injections of fluorescent endothelium–binding SBA lectin and quantified as percentage of lectin-positive vessels over CD31-positive vessels. SBA lectin (green) was found to overlap with anti–CD31-mAb (red) staining on cryosections in islets (dashed lines) transplanted to muscle ($n = 5$, 11 islets) (blue, nuclei, Hoechst 33342) (*D*) and in native islets ($n = 4$, 7 islets) (*E*). Islets transplanted to the liver ($n = 4$, 8 islets) had no functional intraislet vessels (*F*). All values are given as means ± SEM. Bars in *A*, *B*, *D*, *E*, and *F* are 50 μm. post-tx, posttransplantation. (A high-quality digital representation of this figure is available in the online issue.)

tropenic mice resulted in complete inhibition of revascularization of islets 3–5 days posttransplantation (Fig. 3*D* and *E*), and no intraislet vessels could be detected. **Alloxan-induced diabetes is reversed by islets transplantation to muscle or liver, but only muscle engrafted islets show an unaffected response to glucose load.** To investigate the ability of islets transplanted to muscle to regulate blood glucose, recipient mice were rendered diabetic through alloxan treatment, resulting in plasma glucose levels of 25.8 ± 1.0 mmol/l. Thereafter, 300 islets were either transplanted into the abdominal external oblique muscle ($n = 8$) or into the liver ($n = 6$). There was not a difference in time to normalization of blood glucose levels between the two sites; both groups were below 11.1 mmol/l at just over 1 week posttransplantation (Fig. 4*A*). Three mice with plasma glucose levels >20 mmol/l 1 week posttransplantation were killed because of ethical requirements (two with grafts in muscle and one with grafts in the liver). Plasma glucose levels in the successful recipients remained <11.1 mmol/l for at least 2 months. Islet functionality was tested by an intraperitoneal glucose tolerance test. Animals with islets transplanted to muscle did not significantly differ in glucose handling from nondiabetic control mice, but animals with islets transplanted to liver had a significant delay in lowering blood glucose after glucose load (Fig. 4*B*), resulting in an increased

area under the curve (Fig. 4*C*). Islets transplanted to the abdominal external oblique muscle of diabetic mice had vascular densities similar to those of islets transplanted to the cremaster muscle of nondiabetic mice (967 ± 65 vs. 1,162 ± 120 vessels/mm^2) (Fig. 4*D*). Insulin staining of pancreata after termination of experiments confirmed maintained low densities of β-cells in all alloxan-treated mice, excluding the possibility of normalization of blood glucose levels due to β-cell regeneration. The intramuscular site was visualized 3 days after transplantation of fluorescently labeled islets through IVIS imaging (Fig. 4*E*).

Autotransplanted islets to striated muscle of pancreatectomized patients exhibit higher blood flow compared with adjacent muscle tissue. Three pancreatectomized patients receiving autotransplantation of isolated islets to the brachioradialis muscle were scanned using magnetic resonance imaging 3–6 months after surgery. The MRI technique used yields a very high in-plane resolution of 200 μm in vivo (33), which is required to accurately visualize the islet grafts. Islets could indeed be detected in muscle tissue at the site of injection in all three patients (Fig. 5*A*, *C*, *E*, and *F* and supplemental Fig. 5). Therefore, fractional plasma volume, which corresponds to capillary density of the scanned area, was investigated through kinetic modeling. In two of the subjects, the capillary density was assessed through dynamic contrast
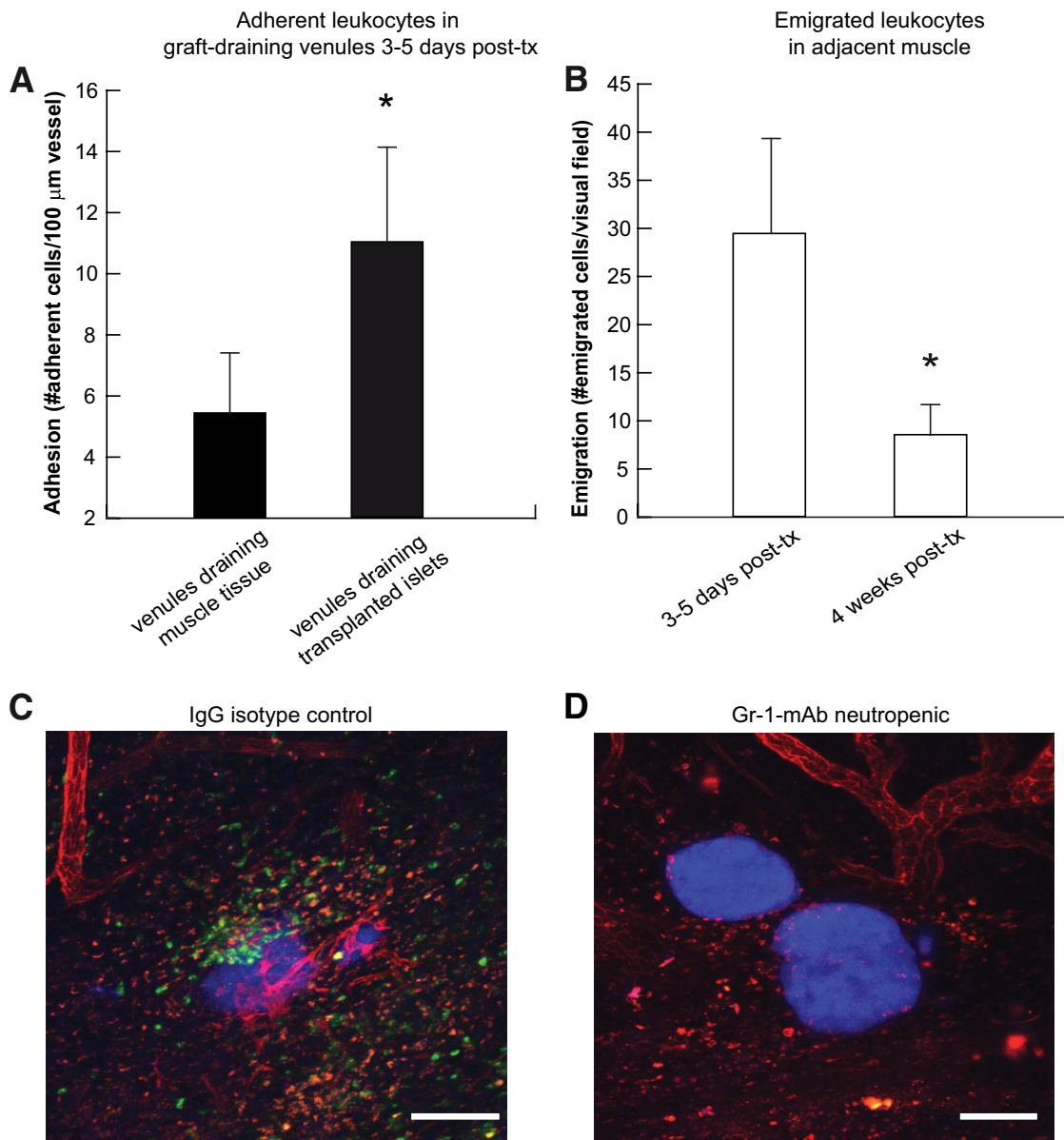
FIG. 3. Islet revascularization in muscle is dependent on neutrophils. *A*: Leukocyte adhesion in venules from mouse cremaster muscle. Three to five days posttransplantation (post-tx), more adherent leukocytes were found in venules draining islets ($n = 5$) than in venules draining only muscle tissue ($n = 5$); *$P = 0.049$. *B*: Leukocyte emigration in the proximity of the transplanted islet was increased at 3–5 days posttransplantation ($n = 5$) compared with 4 weeks posttransplantation ($n = 5$); *$P = 0.042$. *C*: Confocal image of a transplanted mouse islet (blue; Celltracker) 4 days after transplantation to a mouse treated with IgG isotype control antibody, with ingrowing blood vessels (red; anti–CD31-mAb given intra-arterially in vivo) surrounded by leukocytes (green, anti–Gr-1-mAb, given intra-arterially in vivo) in the peritransplant area. *D*: Confocal image of two islets (blue; Celltracker) at 4 days after transplantation transplanted to a neutropenic mouse with no ingrowing blood vessels (red; anti–CD31-mAb given intra-arterially in vivo). All values are given as means ± SEM. Bars in *C* and *D* are 50 μm. (A high-quality digital representation of this figure is available in the online issue.)

enhancement of the equivalent parameter, the plasma volume, and was found to be 2.5 and 3.4 times higher in the implanted clusters of islets compared with the surrounding muscle tissue. The center of the larger islet grafts (Fig. 5*C* and *D*) had a nonperfused area, which most likely corresponds to central fibrosis due to a too-large volume of islets implanted at the same site. Hepatic steatosis has been reported following islet transplantation to the liver (34,35), but no focal lipid accumulation surrounding the muscle-implanted grafts in the first two subjects could be detected (Fig. 5*A* and *C*). Even when high-resolution morphological imaging on the third subject was used, no lipid deposits could be detected close to engrafted islets (Fig. 5*E* and *F*).

DISCUSSION

Transplantation of isolated pancreatic islets to patients suffering from diabetes is limited by loss of function of the grafts, which appears to be related to the site of engraftment (36) including poor revascularization of the islets (17). In the present study we report that vasculature within islets engrafted in striated muscle are functionally and morphologically restored within 2 weeks of transplantation. The results were obtained using intravital and confocal microscopy and by immunohistochemical evaluation and curative transplantations of diabetic mice. Initiation of revascularization was dependent on Gr-1–positive leukocytes recruited to the implantation site; no revasculariza-
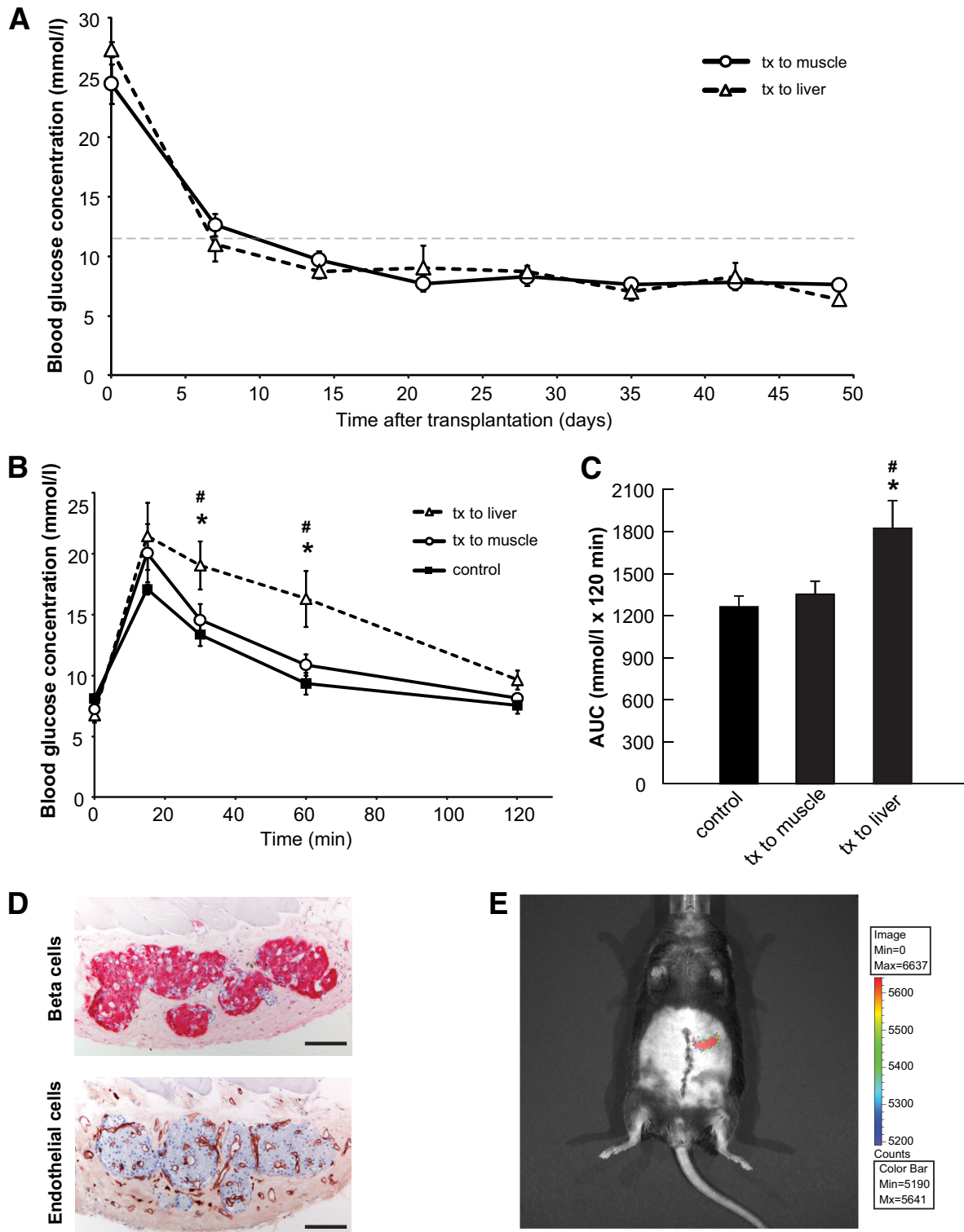
FIG. 4. Islets transplanted to muscle reverse alloxan-induced diabetes. *A*: Plasma glucose levels of mice made diabetic with alloxan and then transplanted with pancreatic islets into the abdominal wall or into the liver at day 0. Plasma glucose levels fell to a stable, normoglycemic level (<11.1 mmol/l) (dashed gray line) within 8 ± 2 days. *B*: Intraperitoneal glucose tolerance test of transplanted mice reaching normoglycemia with islets in muscle ($n = 6$), with islets in the liver ($n = 5$) and nondiabetic control mice ($n = 4$) *$P < 0.05$ control vs. transplantation (tx) to liver. #$P < 0.05$ vs. transplantation to muscle. *C*: Calculated area under the curve from the intraperitoneal glucose tolerance test (*$P = 0.047$ vs. control; #$P = 0.048$ vs. transplantation to muscle). *D*: Tissue sections showing islets engrafted in abdominal muscle with β-cells in red (insulin antibody) and blood vessels in brown (BS-1 lectin). Bars are 50 μm. *E*: Image showing emitted fluorescent light from 300 islets, stained with an intracellular fluorescent probe, and transplanted to the abdominal wall. Max, maximim; Min, minimum. (A high-quality digital representation of this figure is available in the online issue.)

tion of transplanted islets could be observed after depletion of this leukocyte subset. Ultimately, an increased capillary density was detected in islet grafts

compared with adjacent tissue in pancreatectomized patients with isolated islets autotransplanted to muscle using an ultra-high resolution acquisition technique that was
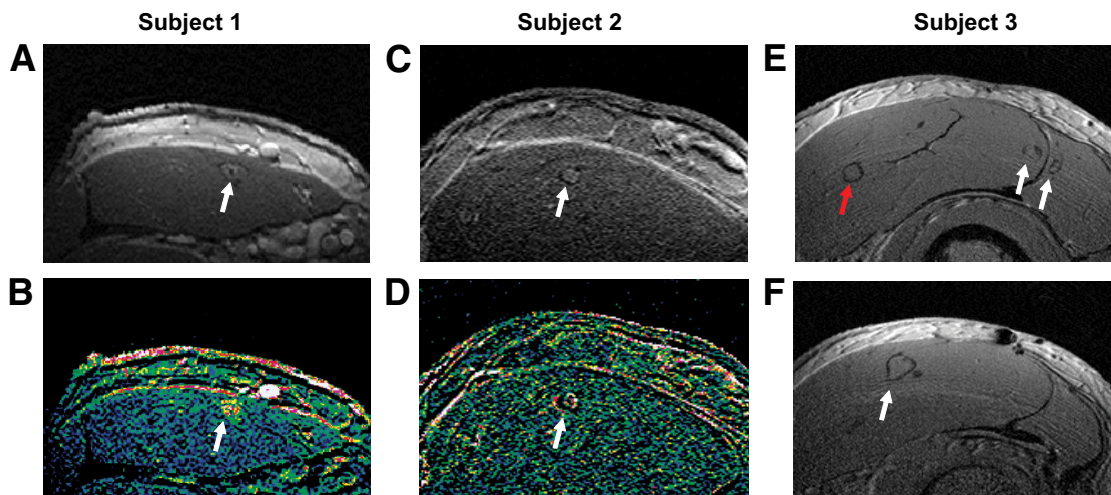
FIG. 5. Higher vessel densities in transplanted islets compared with adjacent muscle in pancreatectomized patients. Axial images of the forearm in three different subjects after islet transplantation (white arrows mark islet grafts). *A* **and** *B*: **Subject 1.** *A*: **Postcontrast.** *B*: **The corresponding plasma volume map calculated from the first pass response. The bright spot in** *B* **is a superficial vein showing very high blood volume.** *C* **and** *D*: **Subject 2.** *C*: **Postcontrast.** *D*: **The corresponding plasma volume map. The increased plasma volume in the islet grafts compared with the surrounding muscular tissue in subjects 1 and 2 are visualized through brighter color markings corresponding to the position of the islets.** *E* **and** *F*: **Two slices from the high-resolution acquisition of subject 3; note the multiple islet grafts. The graft indicated by the red arrow has a diameter of 2.4 mm. (A high-quality digital representation of this figure is available in the online issue.)**

applied to the study of transplanted islets for the first time. This technique enables registration of plasma volumes proportional to capillary densities in small superficial, graft-containing tissue fractions corresponding to transplanted islets. In addition to verifying the experimental observations, this technique will be instrumental during our forthcoming development and evaluation of clinical islet transplantations to the promising muscle site.

Pancreatic islets are highly organized miniature organs with the primary function of regulating blood glucose levels through efficient sensing of present blood glucose concentration and concomitant release of the appropriate hormone (i.e., insulin and glucagon) from each specialized cell type. Justifiably, high blood perfusion and minimal diffusion barriers between the blood, the sensor, and the hormone-releasing cells are prerequisites for efficient blood glucose control (8,9). During isolation, all vascular connections to the islets are interrupted and, contrary to solid organ transplantations, are not reconnected during surgery. Transplanted islets therefore depend completely on revascularization to occur. When islets are grafted into the liver, blood vessels surround the islets but few penetrate the islets (2,17) (supplemental Fig. 1), which may explain the poor long-term function of the grafts. Experimental islet transplantation to other commonly used implantation sites such as the kidney and spleen also results in impaired revascularization (2). Indeed, the present study—where islets were engrafted into striated muscle—reports, for the first time, islet vascular density, vessel morphology, and blood perfusion equal to that of islets in the intact pancreas. These findings were not restricted to the cremaster muscle but could also be seen in islets transplanted to abdominal external oblique, gluteal, and psoas muscles (Fig. 4*D* and supplemental Fig. 4). In addition, the experimental data were confirmed in autotransplanted patients where higher plasma volumes were measured in islets engrafted in forearm muscle compared with adjacent muscle tissue, indirectly demonstrating higher capillary densities in the grafts compared with muscle. Hepatic steatosis of tissue surrounding the grafts has been reported following islet transplantation to the

liver (34,35) due to paracrine insulin effects on adjacent tissue. In the present study, no fat deposits could be detected after autotransplantation to muscle of pancreatectomized patients.

Striated muscle has successfully been used for autotransplantation of parathyroid glands, where these endocrine glands engraft and become vascularized (18). Muscle has also been investigated under experimental settings as a site for pancreatic islet transplantation but with varied success (37–39). The variations in outcome may relate to the techniques used to implant the islets. Indeed, the negative influence of large clusters of islets were evident in the pancreatectomized patients receiving autotransplanted islets to striated muscle: fibrosis could be detected in the center of large number of islets grouped together. In the experimental part of this study, a small volume of 300 nonpacked islets was injected superficially into abdominal muscle in a pearls-on-a-string fashion (39). This resulted in a complete cure of diabetic mice within approximately 8 days following transplantation.

The increased revascularization of islets engrafted in muscle observed in the present study might be dependent on the specific plasticity of the endothelial cell population in muscle. Endothelial cells are heterogeneous, with specialized properties depending on the organ they reside in and their order in the vascular tree. For instance, angiogenesis is induced during a variety of pathologies, but during physiological conditions in adults it is only provoked in ovaries (during ovarian cycling), in the placenta (during placental development), and in muscles (during exercise) (40). Mechanical stretch and increased vessel wall tension during exercise is reported to result in increased capillary supply due to increased local levels of vascular endothelial growth factor (VEGF), hypoxia-inducible factor-1β, and matrix metalloproteinase-2 (41). Thus, a clear difference between striated muscle and other implantation sites investigated for islet vascular densities is that muscle endothelium is programmed to proliferate during muscle overload and concomitant hypoxia (40).

It has recently been reported that leukocytes contribute to angiogenesis occurring during remodeling and healing

of muscle tissue (20,21,42). Hypoxic mediators are known to recruit leukocytes (43,44) and might account for the leukocyte–endothelial cell interactions observed early after islet implantation in this study but not after sham injections. The number of recruited leukocytes decreased with time after transplantation, which parallels islet revascularization and associated reduced hypoxia (45). No revascularization of islets 3–5 days after transplantation could be detected when Gr-1–positive leukocytes had been depleted in recipients, indicating a crucial role of these cells in the angiogenic switch. Gr-1 is reported to be expressed on neutrophils as well as inflammatory monocytes but not on the monocyte population involved in tissue repair (20,42,46). The Gr-1–positive leukocytes recruited to the site of engraftment in the current study that were responsible for initiation of revascularization are therefore most likely neutrophils, while the Gr-1–negative monocyte population that has been shown to be involved in tissue remodeling (21) and tumor angiogenesis (42) does not seem to contribute at these early time points. The mechanism by which neutrophils induce angiogenesis might be release of VEGF—either from intracellular storages or through secretion of matrix metalloproteinase-9, which has been shown to contribute to angiogenesis through digestion of extracellular matrix and release of immobilized VEGF (42).

This study presents a novel paradigm for islet transplantation whereby neutrophils recruited to the site for engraftment were crucial for the functionally restored intraislet blood perfusion following transplantation to striated muscle. In the clinical setting, this site proved to promote islet revascularization and also permitted longitudinal graft monitoring by high-resolution magnetic resonance imaging.

REFERENCES

1. Ryan EA, Paty BW, Senior PA, Bigam D, Alfadhli E, Kneteman NM, Lakey JR, Shapiro AM. Five-year follow-up after clinical islet transplantation. Diabetes 2005;54:2060–2069
2. Mattsson G, Jansson L, Carlsson PO. Decreased vascular density in mouse pancreatic islets after transplantation. Diabetes 2002;51:1362–1366
3. Poitout V, Briaud I, Kelpe C, Hagman D. Gluco-lipotoxicity of the pancreatic beta cell. Ann Endocrinol (Paris) 2004;65:37–41
4. Bennet W, Sundberg B, Groth CG, Brendel MD, Brandhorst D, Brandhorst H, Bretzel RG, Elgue G, Larsson R, Nilsson B, Korsgren O. Incompatibility between human blood and isolated islets of Langerhans: a finding with implications for clinical intraportal islet transplantation? Diabetes 1999;48:1907–1914
5. Moberg L, Johansson H, Lukinius A, Berne C, Foss A, Kallen R, Ostraat O, Salmela K, Tibell A, Tufveson G, Elgue G, Nilsson Ekdahl K, Korsgren O, Nilsson B. Production of tissue factor by pancreatic islet cells as a trigger of detrimental thrombotic reactions in clinical islet transplantation. Lancet 2002;360:2039–2045
6. Redmon JB, Olson LK, Armstrong MB, Greene MJ, Robertson RP. Effects of tacrolimus (FK506) on human insulin gene expression, insulin mRNA levels, and insulin secretion in HIT-T15 cells. J Clin Invest 1996;98:2786–2793
7. Shapiro AM, Gallant HL, Hao EG, Lakey JR, McCready T, Rajotte RV, Yatscoff RW, Kneteman NM. The portal immunosuppressive storm: relevance to islet transplantation? Ther Drug Monit 2005;27:35–37
8. Lifson N, Kramlinger KG, Mayrand RR, Lender EJ. Blood flow to the rabbit pancreas with special reference to the islets of Langerhans. Gastroenterology 1980;79:466–473
9. Lifson N, Lassa CV, Dixit PK. Relation between blood flow and morphology in islet organ of rat pancreas. Am J Physiol 1985;249:E43–E48
10. Samols E, Stagner JI, Ewart RB, Marks V. The order of islet microvascular cellular perfusion is B-A-D in the perfused rat pancreas. J Clin Invest 1988;82:350–353
11. Stagner JI, Samols E. The vascular order of islet cellular perfusion in the human pancreas. Diabetes 1992;41:93–97
12. Stagner JI, Samols E, Bonner-Weir S. Beta––alpha––delta pancreatic islet cellular perfusion in dogs. Diabetes 1988;37:1715–1721
13. Stagner JI, Samols E, Koerker DJ, Goodner CJ. Perfusion with anti-insulin gamma globulin indicates a B to A to D cellular perfusion sequence in the pancreas of the rhesus monkey, Macaca mulatta. Pancreas 1992;7:26–29
14. Nyman LR, Wells KS, Head WS, McCaughey M, Ford E, Brissova M, Piston DW, Powers AC. Real-time, multidimensional in vivo imaging used to investigate blood flow in mouse pancreatic islets. J Clin Invest 2008;118:3790–3797
15. Bonner-Weir S, Orci L. New perspectives on the microvasculature of the islets of Langerhans in the rat. Diabetes 1982;31:883–889
16. Lau J, Mattsson G, Carlsson C, Nyqvist D, Kohler M, Berggren PO, Jansson L, Carlsson PO. Implantation site-dependent dysfunction of transplanted pancreatic islets. Diabetes 2007;56:1544–1550
17. Lau J, Carlsson PO. Low revascularization of human islets when experimentally transplanted into the liver. Transplantation 2009;87:322–325
18. Tominaga Y, Uchida K, Haba T, Katayama A, Sato T, Hibi Y, Numano M, Tanaka Y, Inagaki H, Watanabe I, Hachisuka T, Takagi H. More than 1,000 cases of total parathyroidectomy with forearm autograft for renal hyperparathyroidism. Am J Kidney Dis 2001;38:S168–S171
19. Rafael E, Tibell A, Ryden M, Lundgren T, Savendahl L, Borgstrom B, Arnelo U, Isaksson B, Nilsson B, Korsgren O, Permert J. Intramuscular autotransplantation of pancreatic islets in a 7-year-old child: a 2-year follow-up. Am J Transplant 2008;8:458–462
20. Nahrendorf M, Swirski FK, Aikawa E, Stangenberg L, Wurdinger T, Figueiredo JL, Libby P, Weissleder R, Pittet MJ. The healing myocardium sequentially mobilizes two monocyte subsets with divergent and complementary functions. J Exp Med 2007;204:3037–3047
21. Bryer SC, Fantuzzi G, Van Rooijen N, Koh TJ. Urokinase-type plasminogen activator plays essential roles in macrophage chemotaxis and skeletal muscle regeneration. J Immunol 2008;180:1179–1188
22. Bohman S, Andersson A, King A. No differences in efficacy between noncultured and cultured islets in reducing hyperglycemia in a nonvascularized islet graft model. Diabetes Technol Ther 2006;8:536–545
23. Goto M, Eich TM, Felldin M, Foss A, Kallen R, Salmela K, Tibell A, Tufveson G, Fujimori K, Engkvist M, Korsgren O. Refinement of the automated method for human islet isolation and presentation of a closed system for in vitro islet culture. Transplantation 2004;78:1367–1375

24. Phillipson M, Heit B, Colarusso P, Liu L, Ballantyne CM, Kubes P. Intraluminal crawling of neutrophils to emigration sites: a molecularly distinct process from adhesion in the recruitment cascade. J Exp Med 2006;203:2569–2575

25. Ahren B, Nobin A, Schersten B. Insulin and C-peptide secretory responses to glucagon in man: studies on the dose-response relationships. Acta Med Scand 1987;221:185–190

26. Speier S, Nyqvist D, Cabrera O, Yu J, Molano RD, Pileggi A, Moede T, Kohler M, Wilbertz J, Leibiger B, Ricordi C, Leibiger IB, Caicedo A, Berggren PO. Noninvasive in vivo imaging of pancreatic islet cell biology. Nat Med 2008;14:574–578

27. Nyqvist D, Kohler M, Wahlstedt H, Berggren PO. Donor islet endothelial cells participate in formation of functional vessels within pancreatic islet grafts. Diabetes 2005;54:2287–2293

28. Menger MD, Vajkoczy P, Beger C, Messmer K. Orientation of microvascular blood flow in pancreatic islet isografts. J Clin Invest 1994;93:2280–2285

29. Bonner-Weir S, O'Brien TD. Islets in type 2 diabetes: in honor of Dr. Robert C. Turner. Diabetes 2008;57:2899–2904

30. Cabrera O, Berman DM, Kenyon NS, Ricordi C, Berggren PO, Caicedo A. The unique cytoarchitecture of human pancreatic islets has implications for islet cell function. Proc Natl Acad Sci U S A 2006;103:2334–2339

31. Brissova M, Fowler MJ, Nicholson WE, Chu A, Hirshberg B, Harlan DM, Powers AC. Assessment of human pancreatic islet architecture and composition by laser scanning confocal microscopy. J Histochem Cytochem 2005;53:1087–1097

32. Bosco D, Armanet M, Morel P, Niclauss N, Sgroi A, Muller YD, Giovannoni L, Parnaud G, Berney T: Unique arrangement of α- and β-cells in human islets of Langerhans. Diabetes 59:1202–1210

33. Weis J, Astrom G, Vinnars B, Wanders A, Ahlstrom H. Chemical-shift micro-imaging of subcutaneous lesions. MAGMA 2005;18:59–62

34. Markmann JF, Rosen M, Siegelman ES, Soulen MC, Deng S, Barker CF, Naji A. Magnetic resonance-defined periportal steatosis following intraportal islet transplantation: a functional footprint of islet graft survival? Diabetes 2003;52:1591–1594

35. Bhargava R, Senior PA, Ackerman TE, Ryan EA, Paty BW, Lakey JR, Shapiro AM. Prevalence of hepatic steatosis after islet transplantation and its relation to graft function. Diabetes 2004;53:1311–1317

36. Merani S, Toso C, Emamaullee J, Shapiro AM. Optimal implantation site for pancreatic islet transplantation. Br J Surg 2008;95:1449–1461

37. Stegall MD, Lafferty KJ, Kam I, Gill RG. Evidence of recurrent autoimmunity in human allogeneic islet transplantation. Transplantation 1996;61:1272–1274

38. Axen KV, Pi-Sunyer FX. Long-term reversal of streptozotocin-induced diabetes in rats by intramuscular islet implantation. Transplantation 1981;31:439–441

39. Lund T, Korsgren O, Aursnes IA, Scholz H, Foss A. Sustained reversal of diabetes following islet transplantation to striated musculature in the rat. J Surg Res 2008;160:145–154

40. Prior BM, Yang HT, Terjung RL. What makes vessels grow with exercise training? J Appl Physiol 2004;97:1119–1128

41. Brown MD, Hudlicka O. Modulation of physiological angiogenesis in skeletal muscle by mechanical forces: involvement of VEGF and metalloproteinases. Angiogenesis 2003;6:1–14

42. Nozawa H, Chiu C, Hanahan D. Infiltrating neutrophils mediate the initial angiogenic switch in a mouse model of multistage carcinogenesis. Proc Natl Acad Sci U S A 2006;103:12493–12498

43. Girn HR, Ahilathirunayagam S, Mavor AI, Homer-Vanniasinkam S. Reperfusion syndrome: cellular mechanisms of microvascular dysfunction and potential therapeutic strategies. Vasc Endovascular Surg 2007;41:277–293

44. Weber C, Fraemohs L, Dejana E. The role of junctional adhesion molecules in vascular inflammation. Nat Rev Immunol 2007;7:467–477

45. Olerud J, Johansson M, Lawler J, Welsh N, Carlsson PO. Improved vascular engraftment and graft function after inhibition of the angiostatic factor thrombospondin-1 in mouse pancreatic islets. Diabetes 2008;57:1870–1877

46. Geissmann F, Jung S, Littman DR. Blood monocytes consist of two principal subsets with distinct migratory properties. Immunity 2003;19:71–82